International Journal of Innovative Research in Science, Engineering and Technology (IJIRSET)

| e-ISSN: 2319-8753, p-ISSN: 2320-6710| www.ijirset.com | Impact Factor: 7.512|

||Volume 9, Issue 6, June 2020||

Design and Calibration of a Microcontroller Based Passive Infrared Sensor for Domestic Intruder Detection

Nicodemus M. Sakayo[1], Joseph N. Mutuku[2], James M. Ngaruiya[3]

P.G. Student, Department of Physics, College of Pure &Applied Sciences, JKUAT, Nairobi, Kenya[1]

Associate Professor, Department of Physics, College of Pure & Applied Sciences, JKUAT, Nairobi, Kenya[2]

Senior Lecturer, Department of Physics, College of Pure & Applied Sciences, JKUAT, Nairobi, Kenya[3]

ABSTRACT: The need to secure our homes, commercial complexes, industries and other related properties is of much concern. A home security system should provide security and safety features for a home by alerting the residents from natural and accidental dangers such as; fire, flooding, theft, invading humans and gas leakage. Considering the high rate of crime and insecurity, there is an urgent need to design a high detective security system that takes proper measure to prevent intrusion, unwanted and unauthorized user(s).Microcontrollers play a very vital role in the development and implementation of automation technology. Automation is the process of controlling system and information to decrease the need of human participation and increase accuracy. Home automation represents the idea of controlling of home appliances in an integrated system. The main problem with sensor users in all purposes in the world is the safety and control of using these sensors. Interfacing of the passive infrared sensor with Arduino UNO has been done. The spatial characteristic of a pyro-electric infrared sensor has been investigated at different walking speeds at different distances. This is to design the most appropriate placement point of the PIR sensor for high sensitivity and recognition rate. The PIR sensor performance for infrared radiation detection is high at room temperature. The choice of PIR sensor for the design of unobtrusive activity monitoring system is due to the fact that they are inexpensive and consume very low power. The microcomputer based security system sense the presence of an intruder and alerts the user on the obstruction detected and it also displays the position of the intruder on a screen. A motion sensor detects a change in infrared light intensity and produces a signal which is used to raise an alarm. The optimum values of the sensor has been achieved through calibration of the sensors in the laboratory so as to fit the required environmental conditions. Results obtained are about 90% agreement with the available data acquainted. Correct detection in terms of distance and direction for high recognition rate and the sensors sensitivity method was employed.

KEYWORDS: Passive Infrared (PIR), calibration, intruder, Arduino UNO.

I. INTRODUCTION

Many types of home security systems have been developed. Home or office automation is the control of any or all electrical devices in our homes or offices [2] and is one of the most exciting developments in technology that has come along in decades. In most of the security systems, detectors are used to achieve a secured home or office. Passive infrared detector (PIR) is widely used in presence detectors as a means of human detection [4].

II. RELATED WORK

Various border intrusions detection systems with emphasis on wireless sensor detection methodhave been designed [1]. The systems detect human and non-human intruders such as objects and animals. Thus, their study aimed at ascertaining the intruder crossing a specified border or perimeter under surveillance before raising an alarm. Real-time human identification using a pyroelectric infrared detector array and hidden Markov models was studied by [6]. They noted thatthe identification performance can be improved by increasing the number of detectors and the spatial sampling frequency of the masks. Among all the tested sensor modules, the one containing 8 detector units and a high spatial sampling mask demonstrated the best performance. Its average identification rates for 10 persons are 91% and 78.5%, in path-dependent and path-independent cases, respectively.

Application of pyroelectric infrared sensor (PIR) and the application of processing algorithm in handling sensor information so as to provide real time occupancy map on computer was done by [4]. The PIR sensor was used to detect the presence of human in a protected room. [5] Researched on a low-cost solution for the determination of

characteristic properties of roughly cylindrical objects like size, location, trajectory and velocity of motion, and surface reflectivity. Wireless communications network using frequency modulation technique was developed to handle data transmission through the air. The personal computer played a significant role in providing the intelligent centralized controls of the entire system. A software package was developed for visual display, control mechanism configuration, and embedded server-client application. [9] proposeda model that relates the sensor's analog output waveform to the width of sensing element, and speed of movement and distance of the subject from the PIR sensor.

[3] in their research developed an Arduino® based wireless intrusion detection using infrared (IR) sensor and global system for mobile communication (GSM). This intrusion detection system (IDS) involves a software and hardware tool used to detect unauthorized access a computer system or network. A wireless IDS performs this task exclusively for the wireless network through sensor controlling with different workstations via internet [3]. An IDS usually performs this task in one of two ways: either signature-based or anomaly based detection. Almost every IDS today is at least in part signature-based. Attacks and their tools usually have a unique signature that can be detected and/or found. This means that known attacks can be detected by looking for these signatures. The drawback with these systems is that they are easy to fool and can only detect attacks for which it has a signature. These are not often implemented, mostly because of the high amount of false alarms. An anomaly-based system develops a baseline of what it considers normal traffic. Any time it detects traffic which deviates from what it considers normal an alert is generated. The advantage is that it can catch many attacks that are new or unknown and that would never be seen by signature-based IDS [3].

All objects constantly exchange thermal energy in the form of electromagnetic radiations with their surroundings [11]. The characteristics of the radiations depend on the object and its surroundings' absolute temperature and can be analysed using black body radiations curve governed by Plank's law shown in Equation (2.1)

$$E_{\lambda} = \frac{8\pi\pi h}{\lambda^5} \times \frac{1}{\exp(hc/kT\lambda) - 1} \qquad (2.1)$$

Where *h* isPlanck's constant, *c* is the speed of light , (*k*) is the Boltzmann constant and *T*is absolute temperature. Figure 1 below depicts the Planck's law (coloured curves) accurately described black body.

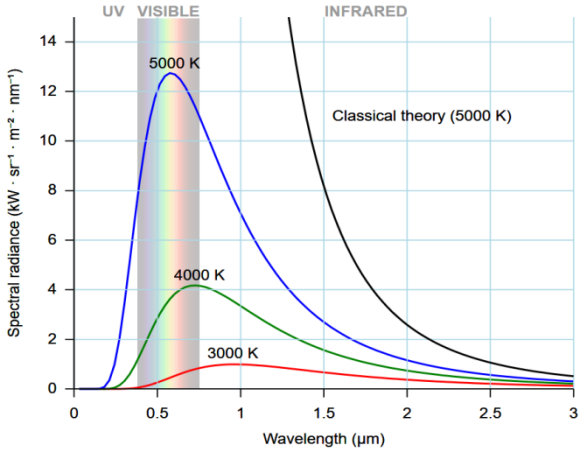

Figure 1: Planck's law (coloured curves) accurately described black body [10]

Human bodies also emit radiation and the wavelength of these radiations can be calculated using Wein's law which is given in equation (2.2),

$$\lambda_{\max}(cm) = \frac{2898}{Temperature(K)} \qquad (2.2)$$

Where λ is wavelength of the emission in nanometre and T is the absolute temperature of the body in K. Substituting T = 310 K (37^0C)normal human body temperature) in (2.2), yields a value for λ of 9348 nm or approximately 10μm. In fact, radiation from the human body is considered to lie in the range of 8-14μm, hence infrared sensors that are sensitive in this range would be able to detect human presence within their detection area.

| e-ISSN: 2319-8753, p-ISSN: 2320-6710| www.ijirset.com | Impact Factor: 7.512|

||Volume 9, Issue 6, June 2020||

2.1 Infrared Sensor Module

Figure 2 below shows the electromagnetic spectrum.

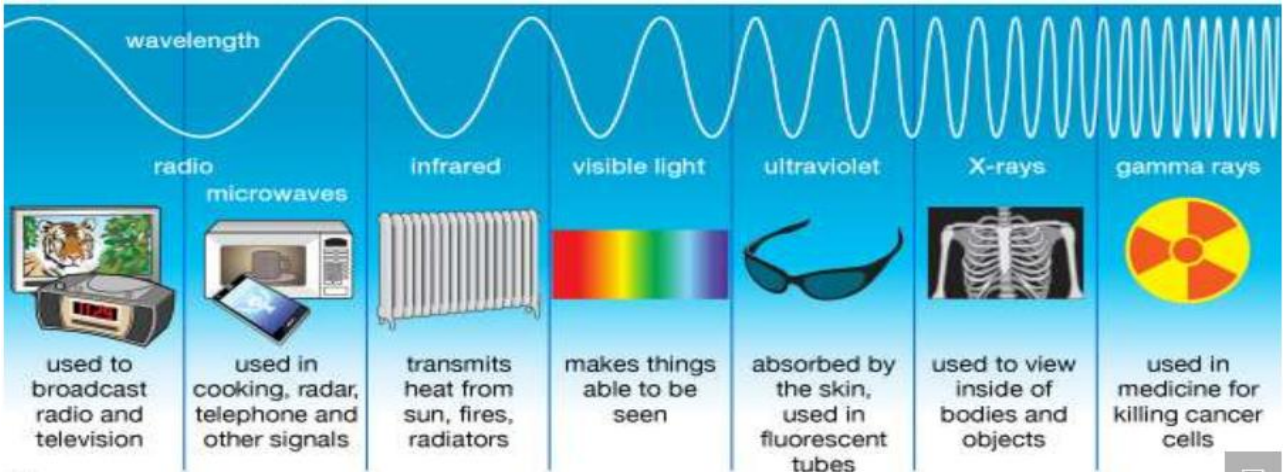

Figure 2: Types of electromagnetic radiation (https://www.britannica.com › science › electromagnetic-spectrum)

Radio waves, infrared rays, visible light, ultraviolet rays, X-rays, and gamma rays are all types of electromagnetic radiation. Infrared radiation exists in the electromagnetic spectrum at a wavelength that is longer than visible light and smaller than microwaves. Infrared radiation cannot be seen but it can be detected. Objects that generate heat also generate infrared radiation including animals and the human body whose radiation is strongest at a wavelength of 9.4 µm.PIR sensors allow one to sense motion, almost always used to detect whether a human has moved in or out of the sensors range. (https://www.elprocus.com)

2.2 The Passive Infrared (PIR) Sensor

Figure 2 below shows the internal schematic diagram. There is a junction gate field-effect transistor (JFET) which has very low-noise and buffers the extremely high impedance of the sensors. The infrared radiation (IR) sensor used in this study is housed in a hermetically sealed metal can to improve noise/temperature/humidity immunity. There is a window made of IR-transmissive material (typically coated silicon since that is very easy to come by) that protects the sensing element. Behind the window are the two balanced sensors.

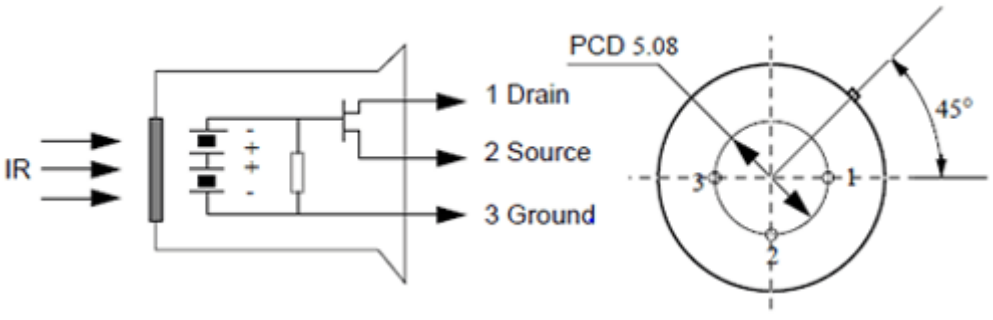

Figure 2: Internal schematic diagram of passive infrared sensor [7]

All PIR modules are characterized by three outgoing cables connected to three PIN placed on the edge of the board.one of the pin is for the power supply **source**, another pin is the ground, and the last is for the detection signal (**drain**). This PIN will emit a signal every time a movement is detected by the PIR sensor.

2.3 Function of PIRs

The PIR is a pyroelectric sensor made of a crystalline material that generates a surface electric charge when exposed to heat in the form of infrared radiation (IR). When the amount of radiation striking the crystal changes, the amount of

charge also changes and can then be measured with a sensitive FET device built into the sensor. The PIR sensor consists of two slots A and B as shown in Figure 3. Each slot is made of a fused silica which is sensitive to IR. When the sensor is idle, both slots will detect the same amount of IR which corresponds to the ambient amount radiated. In case of environmental conditions such as temperature changes and sunlight which affects both elements simultaneously and produce the same amount of output from each element but of opposing polarity and will therefore be cancelled. The sensor produces a change in its output voltage when one of its elements is exposed to a change in radiation as the other is idle.

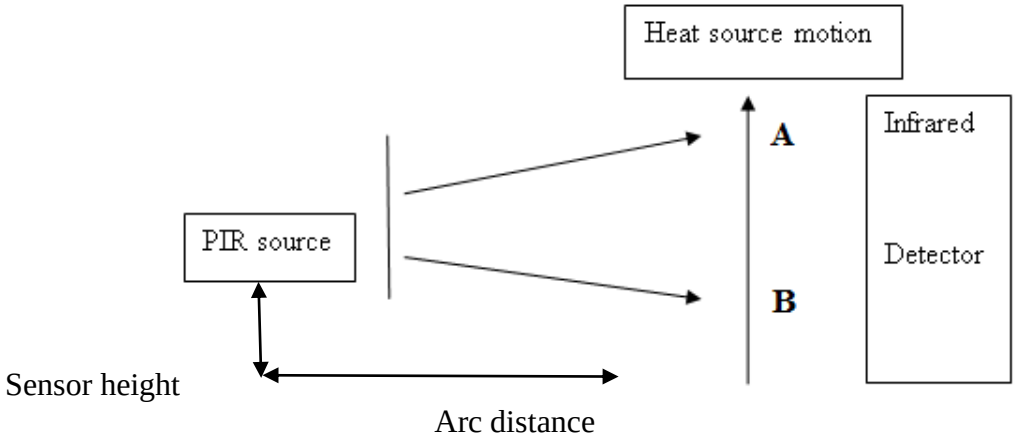

Figure 3: Schematic diagram Illustrating PIR functioning [8]

Once the motion of warm body is detected, a positive differential change between the two slots is detected as a signal and recorded. When the warm body leaves the sensing area, the reverse will happen, whereby the sensor generates a negative differential change which can be detected. These change pulses are what is detected.

2.4 Sensing area coverage

The PIR sensor has a lens which can change the breadth, range, and sensing pattern of the sensor very easily. Usually we'd like to have a detection area that is much larger and allows the infrared radiation to cause a signal in the sensor. When a lens is not used in front of a sensor and an IR emitting body is close to the sensor, about 3 or 4 feet and it moves across the front of the sensor, the radiated IR will expose one element more than the other and a voltage output will result. However, when the IR emitting body is further away from the sensor and its radiation pattern becomes blurred and both elements are exposed more equally, resulting in no voltage output. Placing a lens in front of the sensor extends its detection range. For this reason the sensors are actually Fresnel lenses. The Fresnel lens condenses light, providing a larger range of IR to the sensor. To make it cheaper and affordable we have used a simple lens such as those found in a camera to compare sensitivity and area coverage.

III. METHODOLOGY

This study aimed at assessing the impact of three factors on the proximity and placement point of the PIR sensor for high recognition rate and the sensors sensitivity i.e., the height of sensor location, the vertical distance between the PIR node and movement of the human body, viz: (i) across the detection area at different distances for different walking speeds (ii) walking towards the detector and (iii) walking away from the detector at different angles. The size of the area is 7 m × 7m. The sensors heights are set to 0.5, 1.0, 1.5 and 1.8 m above the ground. Among these heights, 0.5, 1.0, 1.5 and 1.8 m correspond to the part of the human knee, the human hand swing, the human chest and the human head, respectively. In this experiment, the test objects were 5 young adults aged between 25–32 years old. The heights of different human bodies are shown in Table 1. The test objects were required to walk along the predefined six lines marked as A, B, C, D, E and F at different speeds.

| e-ISSN: 2319-8753, p-ISSN: 2320-6710| www.ijirset.com | Impact Factor: 7.512|

||Volume 9, Issue 6, June 2020||

Table 1: Attribute Features of Experiment Object

Object	Height(m)	Step distance (m)
A	1.7	0.5
B	1.74	0.52
C	1.69	0.5
D	1.64	0.41
E	1.6	0.37

As the subject walks through each arc or radial line for the PIR detector, the output from all the objects are recorded. Five analog signals from the detector are sensed and weighted equally. The results considered for the analysis are calculated using equation (3.1).

$$V_i = V_1 + V_2 + V_3 + V_4 + V_5 \quad (3.1)$$

Where V_1, V_2, V_3, V_4 and V_5 are the raw output voltages for objects A, B, C, D and E. The root mean square value of a detector output voltage is calculated over an arc or radial line using equation (3.2).

$$V_i = \sqrt{\frac{\sum_{i=1}^{n} v_i^2}{n}} \quad (3.2)$$

Where $V_i$is the detector output from equation (3.1)over an arc / radial line; and n is the number of detector data points on a given arc/radial line.

IV. EXPERIMENTAL RESULTS

To prove our approach, we recorded several passages for each of the four classes that we wanted to recognize. The results were collected and recorded as tabulated in different tables discussed below.

Table 2: Sensitivity of the PIR sensor placed 0.5 m above the ground for different walking speeds

	Voltage (v)		
Arc radius in meters	**Slow walking**	**Normal walking**	**Fast walking**
1	1.95	1.9	1.42
2	1.96	1.93	1.51
3	1.99	1.98	1.61
4	1.94	1.89	1.58
5	1.82	1.8	1.31
6	1.79	1.73	1.18

Figure 4 below shows the results of voltage against distance for different walking rates.In Figure 4 detector output for slow and normal walking rates between 1 to 3 meters increase with increase in distance. From 3 to 6 meters the output is inversely proportional to distance. This shows that detector sensitivity and recognition rate is quite high when the object is walking at slow speed and in between 1 to 3 meters. The output of fast walking shows detector sensitivity and recognition rate is quite low. The output of all walking rates decrease from 3m to 6 m. This show that the detector sensitivity and recognition rate is quite low as the distance increases from 4 meters.

Table 3 depicts the output when the PIR sensor was at a height of 1.0 m above the ground.

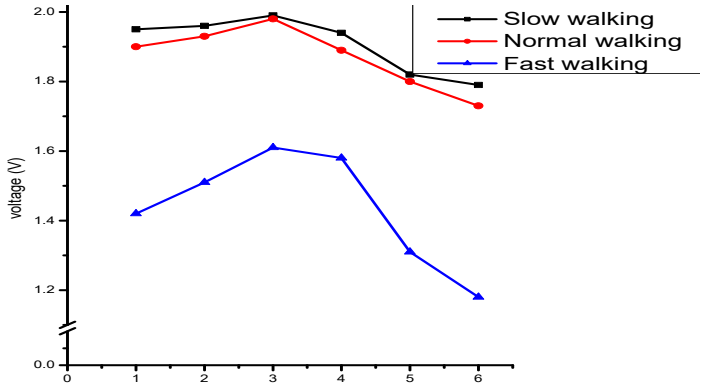

Figure 4: The root mean square value of detector voltage at different distances at different walking speed

Table 3 below shows the Output when the PIR sensor was at a height of 1.0 m above the ground.

Table 3: Output when the PIR sensor was at a height of 1.0 m above the ground.

	Voltage (v)		
Distance in metres (m)	**Slow walking**	**Normal walking**	**Fast walking**
1	2.6	2.55	2.2
2	2.65	2.62	2.25
3	2.8	2.73	2.32
4	2.56	2.48	2.18
5	2.48	2.34	2.13
6	2.36	2.29	2.05

Figure 5 shows the root mean square value of detector voltage at different distances at different walking speeds. Figure 5 shows the output characteristics of the sensor when placed at 1.0 m above the ground. The characteristics of the walking rate curves tend to be similar to the ones of figure 4 but differ with the output values. The detector sensitivity and recognition rate when the sensor is placed at 1.0 meter height is higher compared to when is placed at 0.5 meters. This may be attributed to the hands movement.

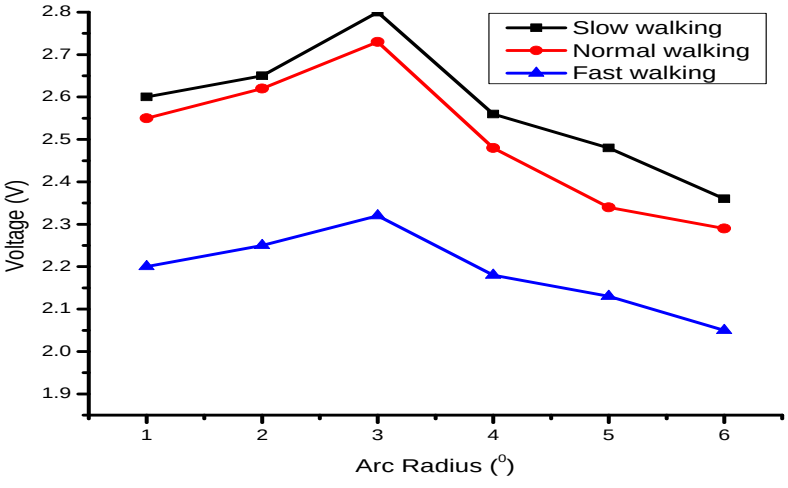

Figure 5: The root mean square value of detector voltage at different distances at different walking speed

Table 4 depicts the results when the PIR sensor was at a height of 1.5 m above the ground.

Table 4: Results when the PIR sensor was at a height of 1.5 m above the ground.

	Voltage (v)		
Arc radius in meters	**Slow walking**	**Normal walking**	**Fast walking**
1	1.99	1.91	1.87
2	2.01	1.96	1.91
3	2.08	2.05	1.93
4	2.04	2.03	1.88
5	2.01	1.96	1.83
6	1.98	1.9	1.82
Mean	**2.018**	**2.038**	**1.920**
Median	**2.020**	**2.050**	**1.905**
Std. deviation	**0.113**	**0.080**	**0.092**

Figure 6 shows the root mean square value of detector voltage at different distances at different walking speed. This shows that detector sensitivity and recognition rate is quite high when the object is walking at slow speed and in between 1 to 3 meters. The output is higher than when the sensor is placed at 0.5 meters but less than when the sensor is placed at 1 meter. This can be attributed to the sufficient time the sensor IR is allowed to interact with the human IR.

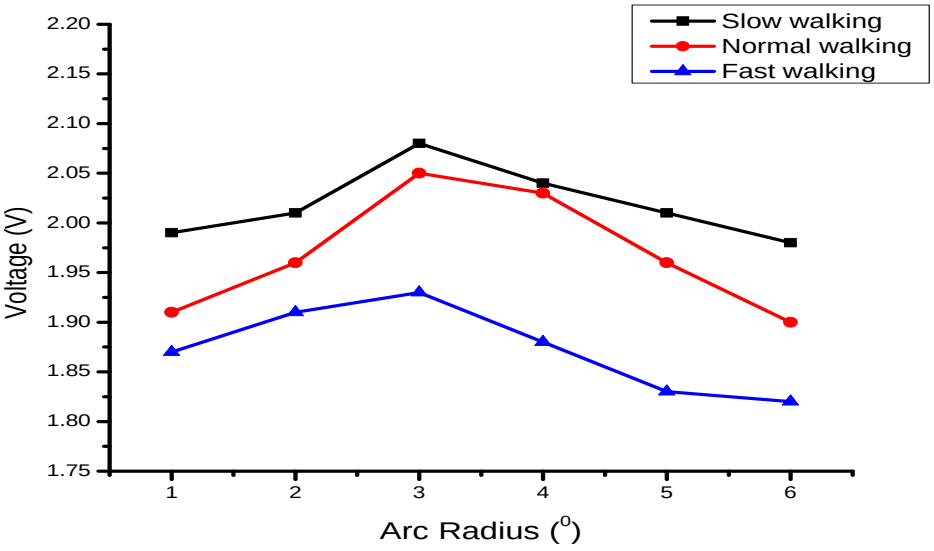

Figure 6: The root mean square value of detector voltage at different distances at different walking speed

Table 5 below shows the results when the PIR sensor was at a height of 1.8 m above the ground

Table 5: Results when the PIR sensor was at a height of 1.8 m above the ground.

	Voltage (V)		
Distance in meters(m)	**Slow walking**	**Normal walking**	**Fast walking**
1	0.99	0.91	0.81
2	1.02	0.98	0.92
3	1.11	1.04	0.99
4	1.16	1.12	1.03
5	1.08	1.11	1.01
6	1.00	1.1	0.98
Mean	**1.060**	**1.043**	**0.957**
Median	**1.05**	**1.07**	**0.985**
Std. deviation	**0.062**	**0.077**	**0.074**

Figure 7 below shows the root mean square value of detector voltage at different distances at different walking speed. The output trend of the sensor placed at 1.8 meters differs with the ones of 0.5, 1.0 and 1.5 meters. This is because it only corresponds to the human head. The detector sensitivity and recognition rate is below 1.2 V hence quite low. The sensitivity for the movements towards and moving away from the detector was tested for slow, normal and fast walking speed.

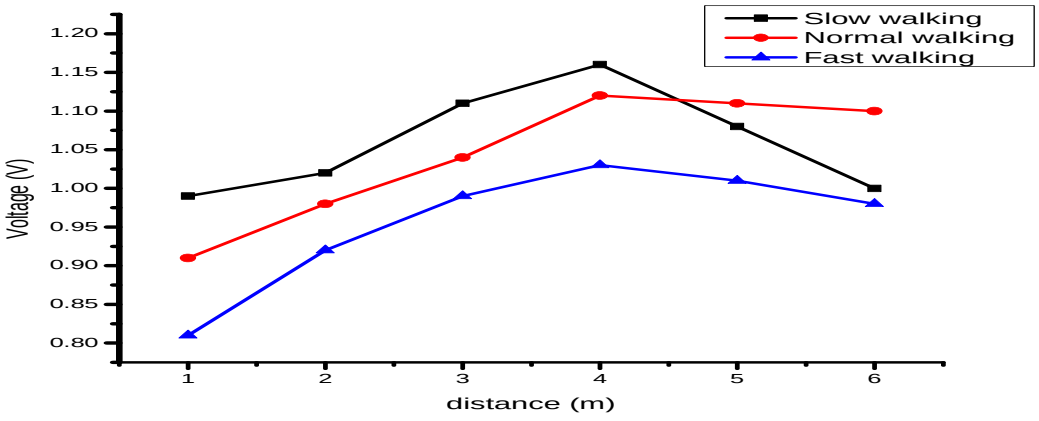

Figure 7: The root mean square value of detector voltage at different distances at different walking speed

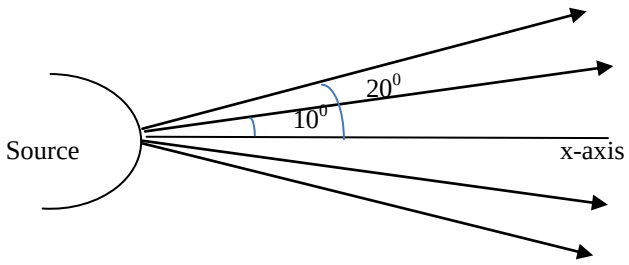

Figure 8: Different walk–away and walk towards arc radius in degrees

Table 6 below depicts walking towards the PIR sensor at different angels. The PIR sensor was positioned at 0.5 m above the ground.

Table 6: Walking towards the PIR sensor at different angels. The PIR sensor was positioned at 0.5 m above the ground.

	Voltage (v)		
Arc radius in degrees	**Slow walking**	**Normal walking**	**Fast walking**
10.00	1.1	1.06	1
20.00	1.21	1.12	1.08
30.00	1.33	1.32	1.16
40.00	1.37	1.34	1.18
50.00	1.38	1.36	1.21
60.00	1.38	1.36	1.22
70.00	1.36	1.34	1.17
80.00	1.27	1.26	1.13
90.00	1.24	1.21	1.05
100.00	1.18	1.12	1.02

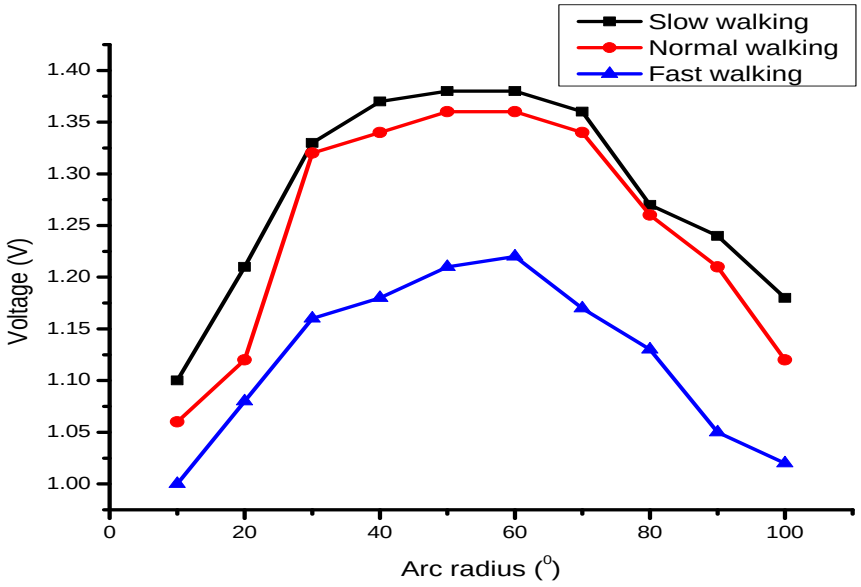

Figure 8: Detector sensitivity at different angles when the subject walked towards the detector at different walking speeds sensor placed at 0.5m

Figures 8 to 11 show detector sensitivities at distance of 0.5m ,1.0 m, ,1.5 m and 1.8 m respectively. It is observed that Figure 8 above shows that the detector sensitivity is relatively constant from 30^{o} to 70^{o} when the movement is towards the detector at slow and normal walking speed and is quite poor at the extreme ends. The highest output of all walking rates is at 50^{o}.The sensor output is reduced for fast walking speed compared to the normal or slow walking. Table 7 below shows walking towards the PIR sensor at different angels. The PIR sensor was positioned at 1.0 m above the ground.

| e-ISSN: 2319-8753, p-ISSN: 2320-6710| www.ijirset.com | Impact Factor: 7.512|

||Volume 9, Issue 6, June 2020||

Table 7 below depicts the Walking towards the PIR sensor at different angels. The PIR sensor was positioned at 1.0 m above the ground.

Table 7: Walking towards the PIR sensor at different angels. The PIR sensor was positioned at 1.0 m above the ground.

	Voltage (v)		
Arc radiation in (^{o})	**Slow walking**	**Normal walking**	**Fast walking**
10	1.12	1.1	1.02
20	1.21	1.18	1.13
30	1.31	1.25	1.18
40	1.34	1.31	1.23
50	1.41	1.38	1.25
60	1.35	1.37	1.22
70	1.3	1.29	1.12
80	1.23	1.19	1.09
90	1.16	1.1	1.01
100	1.12	1.1	1.02
Mean	**1.249**	**1.17**	**0.962**
Median	**1.24**	**1.25**	**1.01**
STDDEV	**0.113**	**0.165**	**0.173**

Figure 9 shows that the detector sensitivity is relatively constant from 30^o to 80^o when the movement is towards the detector at all speeds.

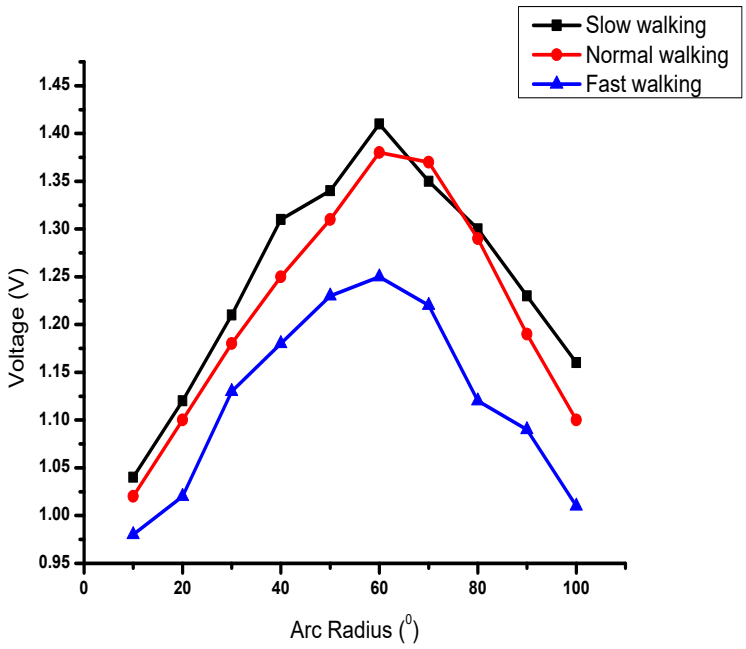

Figure 9: Detector sensitivity at different angles when the subject walked towards the detector at different walking speeds sensor placed at 1m.

Table 8 below shows walking towards the PIR sensor at different angels. The PIR sensor was positioned at 1.5 m above the ground.

Table 8: Walking towards the PIR sensor at different angels. The PIR sensor was positioned at 1.5 m above the ground.

	Voltage (v)		
Arc radiation in cm	**Slow walking**	**Normal walking**	**Fast walking**
10	0.92	0.91	0.87
20	1.03	0.99	0.92
30	1.09	1.15	0.97
40	1.16	1.12	0.98
50	1.18	1.15	0.98
60	1.13	1.1	0.97
70	1.01	1.02	0.92
80	0.94	0.93	0.87
90	0.89	0.9	0.82
100	0.86	0.84	0.79
Mean	**1.102**	**1.024**	**0.805**
Median	**1.09**	**1.1**	**0.86**
STDDEV	**0.114**	**0.165**	**0.174**

Figure 10 shows the root mean square value of detector voltage at different distances at different walking speed. Figure 10 shows that the detector sensitivity overlapping in between the slow and normal speed. This may be attributed to the movement of the hands.The sensor output is reduced for fast walking speed compared to the normal or slow walking.

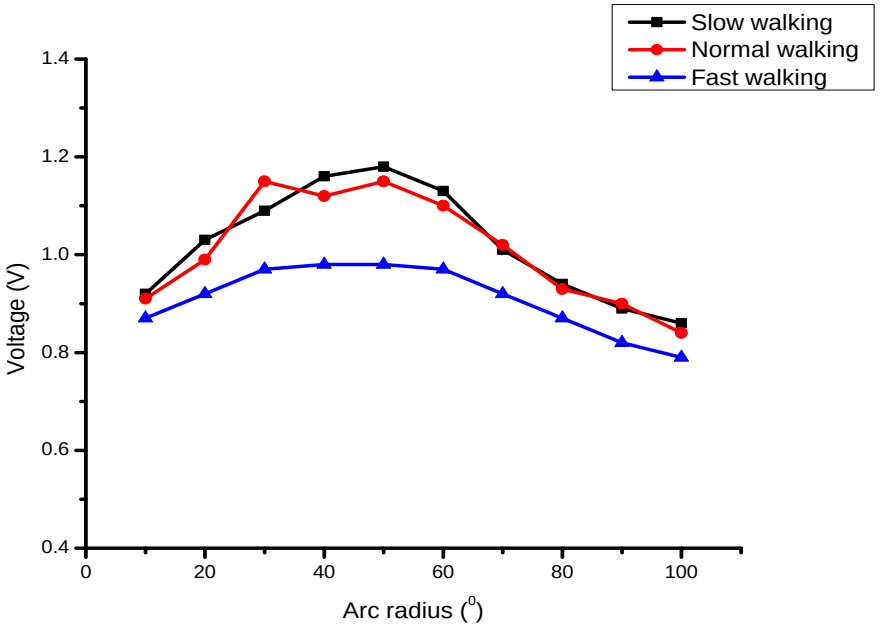

Figure 10: Detector sensitivity at different angles when the subject walked towards the detector at different walking speeds sensor placed at 1.5m.

Table 9 below shows walking towards the PIR sensor at different angels. The PIR sensor was positioned at 1.8 m above the ground.

Table 9: Walking towards the PIR sensor at different angels. The PIR sensor was positioned at 1.8 m above the ground.

	Voltage (v)		
Arc radiation in cm	**Slow walking**	**Normal walking**	**Fast walking**
10	1.25	1.15	0.98
20	0.87	0.87	0.81
30	1.04	1.1	0.9
40	1.11	1.05	0.8
50	1.12	1.1	0.83
60	1.03	1.08	0.94
70	0.89	0.61	0.41
80	0.87	0.75	0.5
90	1.02	1	0.6
100	1.04	1.05	0.75
Mean	**1.024**	**0.976**	**0.752**
Median	**1.035**	**1.05**	**0.805**
STDDEV	**0.116**	**0.167**	**0.180**

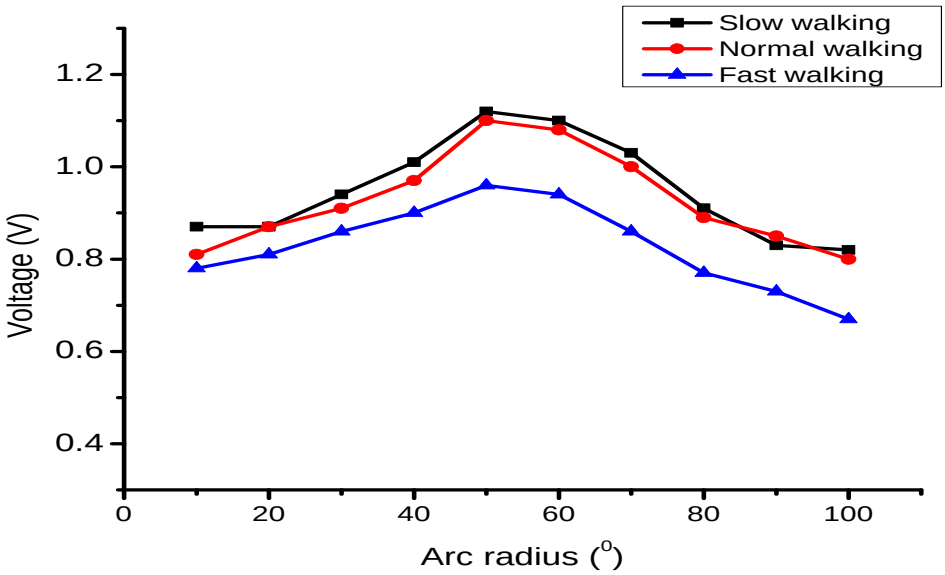

Figure 11: Detector sensitivity at different angles when the subject walked towards the detector at different walking speeds sensor placed at 1.8m.

Figure 11 shows that the detector sensitivity overlapping in between the slow and normal speed. This may be attributed to the fact that it is only the head that has been detected.The sensor output is reduced for fast walking speed compared to the normal or slow walking.

Generally from Figure 8 to Figure 11, as the subject walks through the different arc radius there is general trend of increase and decrease of voltage. The output in slow walking throughout the fig.8 to fig 11 give the highest gradient voltage. This is due to the fact that the source of the infrared radiation and the PIR sensor interact more because of the speed. The maxima is deviating from figure 8 to 11 but ranges between arc radiation of 50^0-60^0 the maxima output is

| e-ISSN: 2319-8753, p-ISSN: 2320-6710| www.ijirset.com | Impact Factor: 7.512|

||Volume 9, Issue 6, June 2020||

1.5m and is when the sensor is placed at 1m above the ground. This is due to the fact that the main body is corresponding directly. As the object walks towards the sensor a general trend of increase of the voltage output is observed.

Table 10 below depicts walking away from PIR sensor at different angels. The PIR sensor was positioned at 0.5 m above the ground.

Table 10 below shows the walking away from PIR sensor at different angels.

Table 10: Walking away from PIR sensor at different angels. The PIR sensor was positioned at 0.5 m above the ground.

	Voltage (v)		
Arc radiation in degrees	**Slow walking**	**Normal walking**	**Fast walking**
10	1.2	1.18	1.13
20	1.23	1.2	1.14
30	1.3	1.26	1.17
40	1.35	1.32	1.21
50	1.36	1.33	1.24
60	1.29	1.29	1.25
70	1.27	1.25	1.18
80	1.26	1.23	1.17
90	1.22	1.17	1.09
100	1.16	1.13	1.06

Figure 12 shows that the detector sensitivity is relatively constant from 20^{o} to 90^{o} when the movement is towards the detector at all speeds. Since the start point is at the sensor, this may affect the amount of radiation being detected throughout. The sensor output is slightly low for fast walking speed compared to the normal or slow walking.

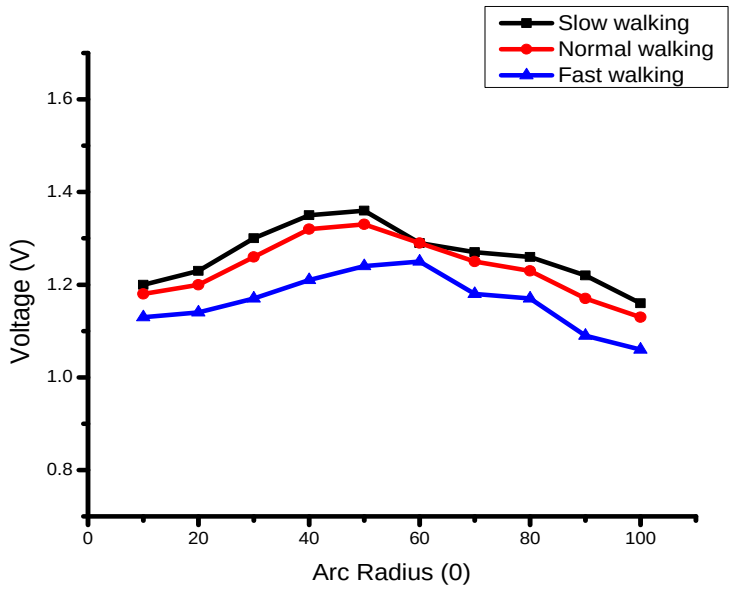

Figure 12: Walking away from PIR sensor at different angels. The PIR sensor was positioned at 0.5 m above the ground.

Table 11 below shows walking away from PIR sensor at different angels. The PIR sensor was positioned at 1.0 m above the ground.

Table11: Walking away from PIR sensor at different angels. The PIR sensor was positioned at 1.0 m above the ground.

	Voltage (v)		
Arc radiation in ^{0}	**Slow walking**	**Normal walking**	**Fast walking**
10	1.25	1.26	1.16
20	1.32	1.28	1.17
30	1.38	1.36	1.21
40	1.43	1.39	1.3
50	1.45	1.41	1.37
60	1.46	1.42	1.36
70	1.41	1.39	1.29
80	1.39	1.35	1.2
90	1.35	1.29	1.19
100	1.29	1.24	1.2
Mean	**1.35**	**1.29**	**1.21**
Median	**1.34**	**1.34**	**1.20**
STD DEV	**0.1299**	**0.1636**	**0.0773**

Figure 13 shows that the detector sensitivity being erupt. Despite the start point being near the sensor, the hands movement seem to contribute a high percentage in the output.

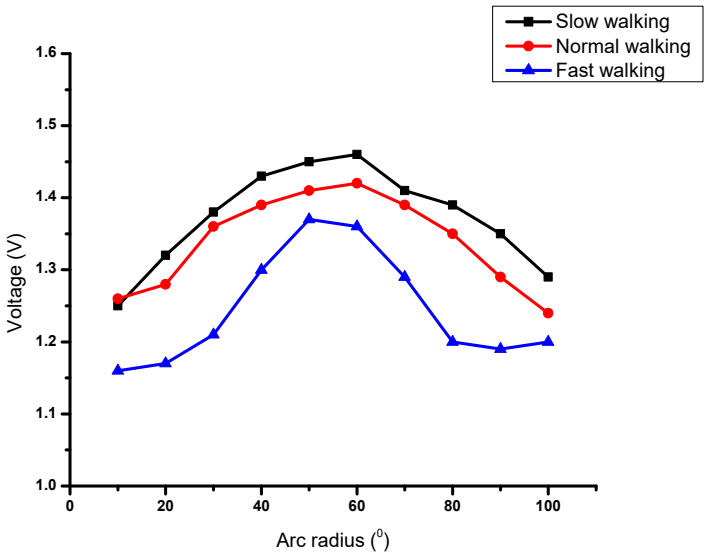

Figure 13: Walking away from PIR sensor at different angels. The PIR sensor was positioned at 1.0 m above the ground

| e-ISSN: 2319-8753, p-ISSN: 2320-6710| www.ijirset.com | Impact Factor: 7.512|

||Volume 9, Issue 6, June 2020||

Table 12 below depicts walking away from PIR sensor at different angels. The PIR sensor was positioned at 1.5 m above the ground.

Table 12: Walking away from PIR sensor at different angels. The PIR sensor was positioned at 1.5 m above the ground.

	Voltage (v)		
angle(°)	**slow walking**	**normal walking**	**fast walking**
10	1.02	0.98	0.89
20	1.07	1.03	0.94
30	1.1	1.04	0.98
40	1.15	1.12	1
50	1.21	1.18	1
60	1.27	1.23	1.07
70	1.23	1.19	1.1
80	1.19	1.18	1.02
90	1.11	1.04	0.98
100	1.09	1	0.92

Figure 14 below depicts the Walking away from PIR sensor at different angels. The PIR sensor was positioned at 1.5 m above the ground

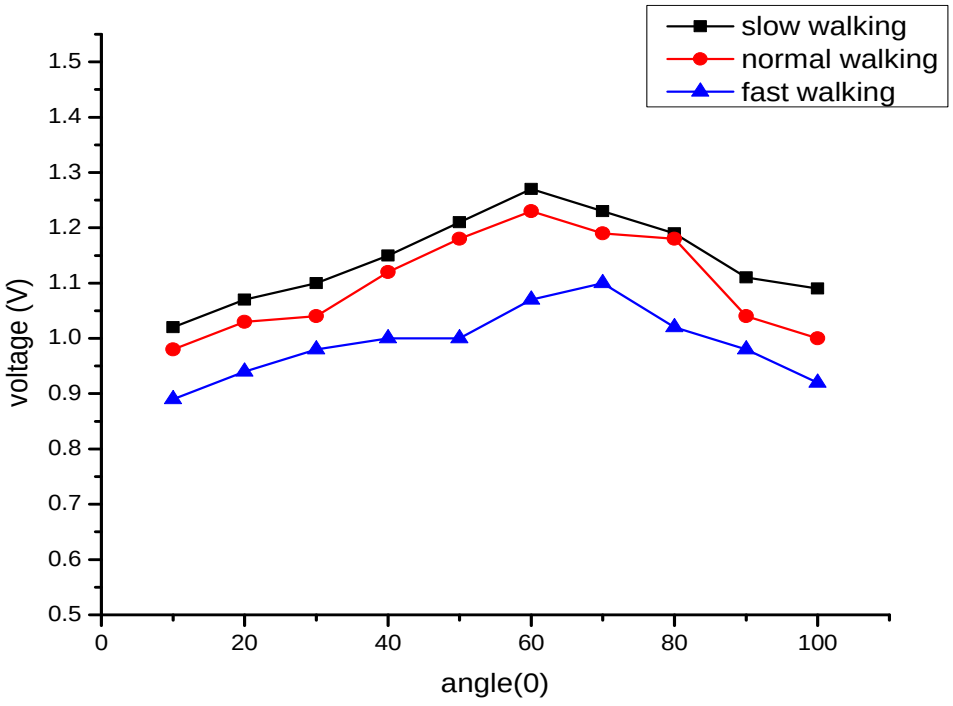

Figure 14: Walking away from PIR sensor at different angels. The PIR sensor was positioned at 1.5 m above the ground

Table 13 below shows walking away from PIR sensor at different angels. The PIR sensor was positioned at 1.8 m above the ground**.**

Table 13: Walking away from PIR sensor at different angels. The PIR sensor was positioned at 1.8 m above the ground.

	Voltage (v)		
Arc radiation in ^{0}	**Slow walking**	**Normal walking**	**Fast walking**
10	0.8	0.68	0.48
20	0.84	0.76	0.51
30	0.87	0.79	0.58
40	0.91	0.82	0.63
50	0.92	0.86	0.65
60	1	0.89	0.7
70	0.99	0.87	0.67
80	0.93	0.79	0.62
90	0.89	0.74	0.59
100	0.86	0.69	0.53
Mean	**1.004**	**1.145**	**0.986**
Median	**1.03**	**1.19**	**1**
STDDEV	**0.169**	**0.164**	**0.124**

Figure 15 below shows the Walking away from PIR sensor at different angels. The PIR sensor was positioned at 1.8 m above the ground. Smooth curves tend to be realized. The speed seem to offer the difference in output. This may be attributed to the fact that it is only the head that has been detected.

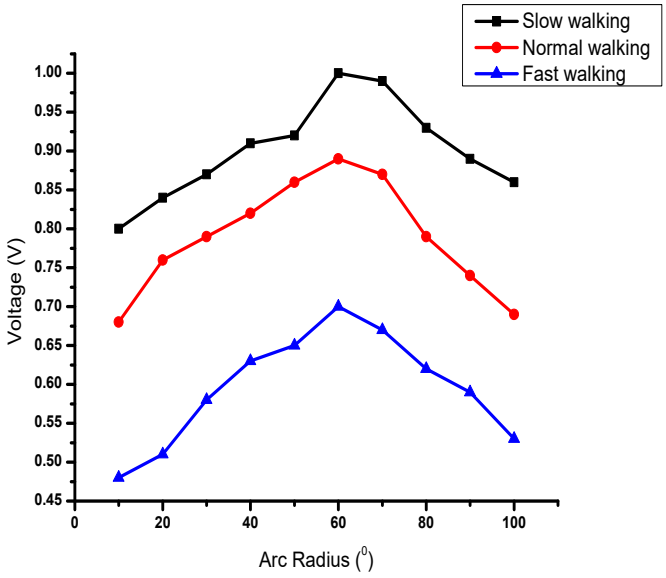

Figure 15: Walking away from PIR sensor at different angels. The PIR sensor was positioned at 1.8 m above the ground

From Figure 12 to Figure 13 shows the trend of increase and decrease of the voltage output. The maxima arc radiation range is 55^0-60^0 .The y-intercept range is below the curves of the walk towards. The maxima is at 1.46 V. This difference may be attributed to the body direction.

| e-ISSN: 2319-8753, p-ISSN: 2320-6710| www.ijirset.com | Impact Factor: 7.512|

||Volume 9, Issue 6, June 2020||

In both cases, (object walking away and towards) there is an increase of the voltage output, but the object walking towards is greater than walking away.

V. CONCLUSION

The spectrum of a single PIR sensor's temporal signal (analog feature) is used to represent the human motion features. Decreased sensitivity to walking speeds, is been realized. The higher the speed the less the chances of being detected. The identification performance can be improved by increasing the number of detectors and proper spatial sampling frequency.

REFERENCES

[1] Alkhathami M., Alazzawi L., and Elkateeb A. (2015). Model and Technique analysis of boarder intrusion detection systems. *Global journal of researchers in engineering* 15(7):1-11

[2] Kaur I. (2010). Microcontroller Based Home Automation System with Security, *International Journal of Advanced Computer Science and Applications*,**1**, (6), 2360-2363

[3] Kumar P., and Kumar P. (2013). Arduino based wireless intrusion detection using IR sensor and GSM. *International Journal of computer science and mobile computing*. 2(5):417-424

[4] Moghavvemi M., and Seng L. (2004). Pyroelectric infrared sensor for intruder detection in Malaysia. *Department of electrical and Telecommunications Engineering. Proceedings of November 21-24,* University of Malaysia, Malaysia, 656-659

[5] Vladislav Pavlov, Heinrich Ruser, and Michael Horn (2007) Feature extraction from an infrared sensor array for localization and surface recognition of moving cylindrical objects. *Institute for Measurement and Automation* University of Bundeswehr Munich, D-85577 Neubiberg, Germany.

[6] Fang, J. S., Hao, Q., Brady, D. J., Guenther, B. D., & Hsu, K. Y. (2006). Real-time human identification using a pyroelectric infrared detector array and hidden Markov models. *Optics express*, *14*(15), 6643-6658.

[7] https://learn.adafruit.com
https://en.wikipedia.org/wiki/Passive_infrared_sensor

[9] BodhibrataMukhopadhyay, SeshanSrirangarajan, SubratKar (2018) Modeling the analog response of passive infrared sensor*Department of Electrical Engineering*, Indian Institute of Technology Delhi, New Delhi, India

[10] https://en.wikipedia.org/wiki/Black_body

[11] Kaushik, A. R. (2006). Characterization of passive infrared sensors for monitoring occupancy pattern. In *2006 International Conference of the IEEE Engineering in Medicine and Biology Society* (pp. 5257-5260). IEEE.

[12] https://www.elprocus.com

[13] https://www.britannica.com › science › electromagnetic-spectrum